Hindawi
Journal of Nanomaterials
Volume 2019, Article ID 2472964, 11 pages
https://doi.org/10.1155/2019/2472964

Research Article

Biocompatible and Biodegradable Electrospun Nanofibrous Membranes Loaded with Grape Seed Extract for Wound Dressing Application

Danilo A. Locilento,[1,2] Luiza A. Mercante,[1,3] Rafaela S. Andre,[1] Luiz H. C. Mattoso,[1,3] Genoveva L. F. Luna,[4] Patricia Brassolatti,[4] Fernanda de F. Anibal,[4] and Daniel S. Correa[1,2]

[1]*Nanotechnology National Laboratory for Agriculture (LNNA), Embrapa Instrumentação, 13560-970 São Carlos, SP, Brazil*
[2]*PPGQ, Department of Chemistry, Center for Exact Sciences and Technology, Federal University of São Carlos (UFSCar), 13565-905 São Carlos, SP, Brazil*
[3]*PPG-CEM, Department of Materials Engineering, Center for Exact Sciences and Technology, Federal University of São Carlos (UFSCar), 13565-905 São Carlos, SP, Brazil*
[4]*Laboratory of Parasitology, Department of Morphology and Pathology, Universidade Federal de São Carlos (UFSCar), 13565-905 São Carlos, SP, Brazil*

Correspondence should be addressed to Luiza A. Mercante; lamercante@gmail.com
and Daniel S. Correa; daniel.correa@embrapa.br

Received 28 August 2018; Revised 29 October 2018; Accepted 4 November 2018; Published 6 March 2019

Academic Editor: Ruibing Wang

The development of nanofibrous membranes with tunable wettability, degradation, and biocompatibility is highly keen for biomedical applications, including drug delivery and wound dressing. In this study, biocompatible and biodegradable nanofibrous membranes with antioxidant properties were successfully prepared by the electrospinning technique. The membranes were developed using polylactic acid (PLA) and polyethylene oxide (PEO) as the matrix, with the addition of grape seed extract (GSE), a rich source of natural antioxidants. The nanofibrous membranes were thoroughly characterized both from the materials and from the biocompatibility point of view. PLA and PLA/PEO nanofibers showed high encapsulation efficiency, close to 90%, while the encapsulated GSE retained its antioxidant capacity in the membranes. *In vitro* release studies showed that GSE diffuses from PLA/GSE and PLA/PEO/GSE membranes in a Fickian diffusion manner, whose experimental data were well fitted using the Korsmeyer-Peppas model. Furthermore, a higher controlled release of GSE was observed for the PLA/PEO/GSE membrane. Moreover, culturing experiments with human foreskin fibroblast (HFF1) cells demonstrated that all samples are biocompatible and showed that the GSE-loaded PLA/PEO nanofibrous membranes support better cell attachment and proliferation compared to the PLA/GSE nanofibrous membranes, owing to the superior hydrophilicity. In summary, the results suggested that the GSE-loaded membranes are a promising topical drug delivery system and have a great potential for wound dressing applications.

1. Introduction

Natural bioactive phenolic compounds have gained much importance in the past years for promoting health or preventing disease due to their beneficial physiological properties, including antioxidant [1–3], anti-inflammatory [4, 5], anticarcinogenic [6–8], and antimicrobial activities [3, 8]. Sources for obtaining polyphenolic compounds are varied, including byproducts and wastes generated by agroindustry [9], which can be used, for instance, as food antioxidants

and antimicrobial agents [10]. In particular, grape seed extract (GSE), a mixture of polyphenols extracted from seeds of wine grapes, has demonstrated superior ability in scavenging free radicals, being 20–50 times more efficient than vitamin E or C [2, 11].

Despite the wide spectrum of properties, the use of these compounds has been limited in the pharmaceutical field [12], due to the poor water solubility and high chemical instability in physiological medium, which results in poor bioavailability, low permeability, and degradation before reaching the systemic circulation [12–14]. One way to tackle these issues is to entrap/adsorb these molecules in/onto biobased polymer matrices. In this context, electrospinning has been established as an outstanding technique to entrap bioactive compounds within polymer matrices aiming to be used for drug delivery and wound dressing applications [15–18]. Recently, electrospun nanofibers have been proposed for stabilizing and controlling the release of various bioactive compounds, such as caffeic acid [8], *Centella asiatica* [19], and *Garcinia mangostana* extract [1]. However, little attention has been given to the study and application of electrospinning for the encapsulation of GSE aiming at biomedical applications.

The advantageous properties related to nanoscale dimensions of electrospun nanofibers (NFs) provide a possibility to control/extend the delivery of bioactive molecules to the wound site as well as to improve cell adhesion and proliferation [16, 17]. Such systems are capable of mimicking the extracellular matrix of the various biological tissues, which can improve the biological performance of these membranes [20–24].

Among the biobased polymers, polylactic acid (PLA) is an FDA approved and widely used material in biomedical applications due to the combination of biocompatibility and biodegradability, adequate mechanical strength, and thermal stability [25, 26]. However, PLA is rather hydrophobic, and bulk or surface modification is required to modulate its surface wettability aiming at enhancing biorelated applications. In bulk modification, the addition of hydrophilic polymers, such as polyethylene oxide (PEO), effectively allows for the modulation of biodegradation and drug release kinetics, which are important parameters for wound dressing applications [22, 27].

Herein, we report the design and fabrication of biocompatible nanofibrous membranes with antioxidant properties by means of electrospinning using PLA and PLA/PEO as polymer matrices and GSE as antioxidant compound, as illustrated in Scheme 1. The effects of the nanofiber composition (without/with PEO) on the morphological, chemical, thermal, and *in vitro* biodegradability properties of the final membranes were investigated. Then, both PLA and PLA/-PEO were loaded with GSE and electrospun to produce bead-free smooth nanofibers. Our results demonstrated that the *in vitro* GSE release profile from the nanofibrous membranes can be modulated by appropriate selection of the polymer material composition. Furthermore, the antioxidant activity of the nanofibrous membranes and their biocompatibility were also evaluated through *in vitro* tests using fibroblasts aiming at biomedical and healthcare applications.

2. Experiment

2.1. Materials. Polylactic acid (PLA, MW = 119,000 g mol^{-1}) was obtained from NatureWorks Ingeo®. Polyethylene oxide (PEO, MW = 100,000 g mol^{-1}), 3,4,5-trihydroxybenzoic acid hydrate (gallic acid monohydrate), and 2,2-diphenyl-1-picrylhydrazyl (DPPH) were purchased from Sigma-Aldrich. *N*,*N*-Dimethylformamide (DMF), acetone, Na_2HPO_4, and NaH_2PO_4 were purchased from Synth Chemical (São Paulo, Brazil). The grape seed extract (GSE, polyphenols > 96%) was obtained from Galena (São Paulo, Brazil).

2.2. Preparation of Electrospun Nanofibrous Membranes. PLA and PLA/PEO (9 : 1, *w*/*w*) solutions in DMF/acetone (1 : 1, *v*/*v*) were prepared in optimized condition using a concentration of 9% (*w*/*v* in respect to the solvent mixture) and stirred for 3 h at room temperature. GSE was added to PLA and PLA/PEO solutions at the concentration of 10% (*w*/*w*), with respect to the polymer content, to produce PLA/GSE and PLA/PEO/GSE solutions.

All nanofibrous membranes were fabricated using the same experimental conditions with a homemade electrospinning apparatus operating at a feed rate of 1.0 mL h^{-1} using an electric voltage of 17 kV. A working distance of 9 cm was kept between the syringe and the metallic collector. A steel needle of 0.8 mm (inner diameter) was employed. The experiments were performed at the relative humidity and temperature of 35%±5% and 25°C ± 2°C, respectively.

2.3. Physicochemical Characterization. The morphology and size of the as-prepared nanofibers were evaluated by scanning electron microscopy (SEM, JEOL 6510), with the nanofiber diameter being estimated with the aid of the software ImageJ (National Institutes of Health, USA). In each experiment, the nanofiber average diameter and distribution were determined by measuring 100 random fibers using representative micrographs.

Fourier transform infrared (FTIR) spectra of samples were recorded using a Bruker Vertex 70 equipment. The spectra were collected in ATR mode from 4000 cm^{-1} to 600 cm^{-1}. A total of 64 scans were collected at a resolution of 2 cm^{-1}.

Thermogravimetric (TG) analyses were performed on a thermogravimetric analyzer (Q500 TA Instruments) under air atmosphere, at a flow rate of 20 mL min^{-1}. Samples in platinum pans were scanned from room temperature up to 700°C at a heating rate of 10°C min^{-1}.

Contact angles of PBS buffer (pH 7.4) droplets on the surface of the nanofibers were measured using a contact angle measuring system (CAM 101 model KSV Instruments) equipped with a CCD camera (KGV-5000). For each measurement, a 5 μL droplet was pipetted onto the membrane surface, and the images of the droplet were automatically taken as a function of time. From these images, contact angle values were calculated using dedicated software (KSV CAM 2008).

2.4. Degradation Study. Hydrolytic degradation of the membranes was carried out in phosphate buffer solution

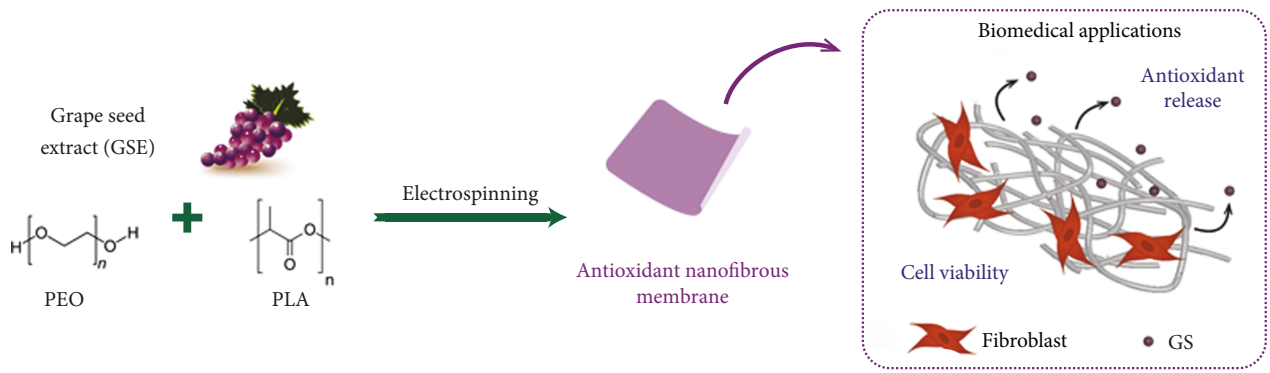

Scheme 1: Schematic representation of preparation of GSE encapsulated into nanofibrous membranes and *in vitro* studies aiming at wound dressing applications.

(pH = 7.4, 37°C) up to 5 weeks, according to methodology described in [28]. At fixed times, i.e., 7, 14, 21, 28, and 35 days, the membranes were taken out from the medium and characterized regarding morphological changes and weight loss after washing with distilled water and vacuum drying.

2.5. Encapsulation Efficiency. Encapsulation efficiency (EE) was determined according to the method previously reported by Chuysinuan et al. [29]. PLA/GSE and PLA/PEO/GSE nanofibrous membranes (around 6 mg) were dissolved in DMF/acetone (1 : 1, *v*/*v*) mixture. The actual amount of the as-loaded GSE was then quantified using UV-Vis absorption spectroscopy (Shimadzu UV-1100) by monitoring the wavelength at 280 nm against a predetermined calibration curve of the extract [30]. Neat PLA and PLA/PEO solutions using the same solvent mixture were used as blanks. Each assay was carried out in triplicate. Finally, the EE was calculated by the following:

$$\text{EE}\,(\%) = \frac{\text{GSE concentration onnanofibers}}{\text{theorical GSE concentration}} \times 100. \quad (1)$$

2.6. Antioxidant Activity. The *in vitro* antioxidant activity of the GSE-loaded nanofibers was evaluated using the DPPH radical scavenging activity assay [31]. The nanofibers were first dissolved in DMF/acetone (1 : 1, *v*/*v*) and treated with a methanolic solution of DPPH (0.1 mM) for 30 min at room temperature in darkness. At the end of 30 min, the absorbance of the solution at 517 nm was measured (Shimadzu UV-1100). The antioxidant activity (AA) of samples was calculated using the following:

$$\text{AA}\,(\%) = \frac{\left(A_{\text{control}} - A_{\text{sample}}\right)}{A_{\text{control}}} \times 100, \quad (2)$$

where A_{control} and A_{sample} are the absorbance values of the DPPH solution without and with the presence of the sample solutions, respectively. The measurements were carried out in triplicate.

2.7. GSE Release Profile and Mechanism Investigation. The *in vitro* release profile study of GSE from PLA and PLA/PEO nanofibers was carried out in a phosphate saline solution (PBS), which simulates blood plasma conditions and/or exudate from a wound [32]. The PLA/GSE and PLA/PEO/GSE membranes (~6 mg) were immersed in 15 mL of PBS (0.1 mol L^{-1}, pH 7.4) at 37°C under mild stirring. Then 2 mL of the solution was taken at specific time intervals and analyzed by UV-Vis absorption spectroscopy (Shimadzu UV-1100) at 278 nm. Meanwhile, the same volume of PBS solution was added to keep the volume constant. The amount of GSE released over time was calculated using the prebuilt calibration curve for GSE in PBS buffer (pH 7.4). The presented data were average values from three measurements. The cumulative release was calculated using

$$\text{Cumulative release}\,(\%) = \left(\frac{M_t}{M_0}\right) \times 100, \quad (3)$$

where M_t (mg) is the mass of GSE released at certain time t and M_0 (mg) is the GSE mass encapsulated in the nanofibers.

The Korsmeyer-Peppas equation [33] was used to describe the GSE release profile from the nanofibrous membranes as follows:

$$\frac{M_t}{M_\infty} = kt^n, \quad (4)$$

where M_t (mg) and M_∞ (mg) are the mass of GSE released at an arbitrary time t and at equilibrium, respectively, k is the release rate constant, and n indicates the release exponent suggesting the nature of the release mechanism [34]. Data acquired from *in vitro* drug release studies were plotted as log cumulative percentage drug release versus log time. Thus, the release mechanism was considered based on the n value obtained from the Korsmeyer-Peppas model fitting curve. The n value was determined considering the portion of the release curve that satisfied $M_t/M_\infty < 0.6$ [35].

2.8. Cell Viability Assay. The effect of the different nanofibrous membranes on cell viability was assessed by the MTT ([3-(4,5-dimethyl- thiazol-2-yl)-2,5-diphenyl tetrazolium bromide]) assay. The cell number and viability were evaluated by measuring the mitochondrial-dependent conversion of the yellow tetrazolium salt MTT to purple formazan

crystals by metabolically active cells [36]. The human foreskin fibroblast (HFF1) cells were cultured using Dulbecco's modified Eagle's medium (DMEM), 10% fetal bovine serum, and 1% penicillin–streptomycin solution. The nanofibrous membranes were seeded in 24-well plates at a density of 5×10^4 cells per well and incubated with 5% CO_2 at 37°C. After 24 and 48 h, the medium of each well was replaced by 10% (*v*/*v*) MTT solution and incubated for 4 h. Then, the formed formazan crystals were dissolved in dimethyl sulfoxide, and the optical density was measured with a microplate reader (Multiskan FC, Thermo Scientific®) at the wavelength of 570 nm. The biocompatibility of the nanofibrous membranes was expressed as % cell viability, which was calculated from the ratio between the number of cells treated with the nanofibers and that of nontreated cells (control). Each variant of nanofibrous membrane was assayed by five measurements, and the results were expressed as mean ± standard deviation. Results were analyzed through the one-way analysis of variance (ANOVA) followed by Tukey's test. Statistical significance was set at $p < 0.05$, and the software used was GraphPad Prism 5.0 (San Diego, CA, USA).

SEM images were carried out to evaluate the morphological changes of HFF1 cells on the nanofibrous membranes after 48 hours of cell culture. Firstly, the membranes were washed with PBS to remove nonadherent cells and fixed with Karnovsky's fixative. The samples were then dehydrated through a series of graded ethanol solutions and subsequently dried at room temperature.

3. Results and Discussion

3.1. Nanofibrous Membrane Characterization. The morphology and size of the as-prepared nanofibrous membranes were investigated by SEM images, according to results present in Figure 1 and Table 1. Nanofibers with uniform, smooth, nonporous, and randomly orientated structures were obtained for all formulations. Neat PLA nanofibers (Figure 1(a)) presented a fiber diameter of 149 ± 23 nm. The addition of PEO (Figure 1(b)) increased the fiber diameter (304 ± 46 nm) owing to the free volume increase that occurs on blending the two polymers, which is attributed to the different segmental conformations between the PLA and PEO, reducing the PLA chain–chain packing [37]. As can be seen in Figures 1(c) and 1(d), the addition of GSE did not significantly affect the morphology and diameter of the nanofibers when compared with their counterparts (PLA and PLA/PEO nanofibers).

Figure 2(a) illustrates the FTIR spectra of the GSE extract powder and PLA and PLA/PEO nanofibers unloaded and loaded with the extract. GSE is mainly composed of phenolic compounds, such as procyanidins, catechin, epicatechin, gallic acid, and gallic acid ester [2]. Typical bands of these phenolic compounds can be observed at 3300 cm^{-1} corresponding to stretching modes of the different –OH groups, at 1604 and 1520 cm^{-1} due to the –C=C–O deformation of the heterocyclic ring, at 1437 cm^{-1} attributed to the –CH deformation of the aromatic ring, at 1283 cm^{-1} associated with ester C–O stretching, and at 1104 cm^{-1} due to phenol and ether C–O stretching [34, 38]. The FTIR spectrum of PLA displayed the characteristic carbonyl (C=O) absorption band at 1752 cm^{-1}, the C–O–C stretching bands at 1184 and 1086 cm^{-1}, while the peaks at 1453 and 1382 cm^{-1} are related to the C-H deformation [31]. The PLA/PEO blend nanofibers displayed the characteristics bands of PLA at 1752 (C=O), 1180 and 1082 cm^{-1} (O–C–O), while the C–H stretch from the PEO backbone appeared at 2890 cm^{-1} [37]. After the GSE incorporation, an extra vibrational mode assigned to the –C=C–O deformation of GSE was observed at 1619 and 1616 cm^{-1} for PLA/GSE and PLA/PEO/GSE, respectively (Figure 2(b)). These bands are shifted with respect to the GSE powder, indicating an interaction between the polymeric matrix and the extract, most probably based on intermolecular hydrogen bonds [8, 14, 31]. Regarding the PLA/PEO/GSE nanofibers, an additional peak at 1518 cm^{-1}, characteristic of phenolic compounds, appeared in the spectrum. These results confirm the successful loading of GSE into PLA and PLA/PEO nanofibrous membranes.

Typical thermogravimetric (TG) analysis and derivative (DTG) curves of pure GSE and unloaded and GSE-loaded nanofibers were obtained, and the results are presented in Figure 3. Pristine PLA nanofibers decomposed in a single-stage event between 295 and 370°C. The decomposition onset temperature (T_o) and the temperature at maximum degradation rate (T_{max}) of the blend PLA/PEO membranes shifted from 320 to 270°C and from 360 to 325°C, respectively. The decrease in PLA thermal stability may be attributed to the fact that PEO can intersperse around PLA polymer chains and break polymer-polymer interactions [37, 39]. For powder GSE (Figure 3(b)), the TG curve shows an initial event of mass loss (4%) below 100°C associated with water desorption followed by its decomposition in the range of 120 to 515°C. The DTG curve of the extract displays a large peak in the temperature range of 120-290°C, followed by two other peaks at 430 and 505°C, suggesting that many overlapping processes occur as a consequence of complex composition of grape seeds [40, 41]. TG/DTG curves of PLA/GSE and PLA/PEO/GSE membranes (Figure 3(b)) show two stages of mass loss due to the sequential degradation of the polymeric matrix and GSE. The temperature of the second degradation peak, which corresponds to the degradation temperature of GSE, significantly decreased upon encapsulation, probably due to the dissolution/dispersion of the bioactive compound before encapsulation [42].

The hydrophilicity feature of any material for biomedical applications is a crucial parameter, as it can affect cell adhesion and growth on its surface [43]. The surface hydrophilicity of the nanofibrous membranes was characterized by contact angle measurements. As shown in Table 1, PLA/PEO nanofibers displayed enhanced hydrophilicity compared to isolated PLA nanofibers, corroborating the good strategy of blending polymers. The incorporation of PEO in the matrix introduces preferable sites for aqueous compounds to be attached while retaining the overall structural integrity [5]. In comparison with PLA and PLA/PEO nanofibers, the addition of GSE did not significantly affect their surface wettability.

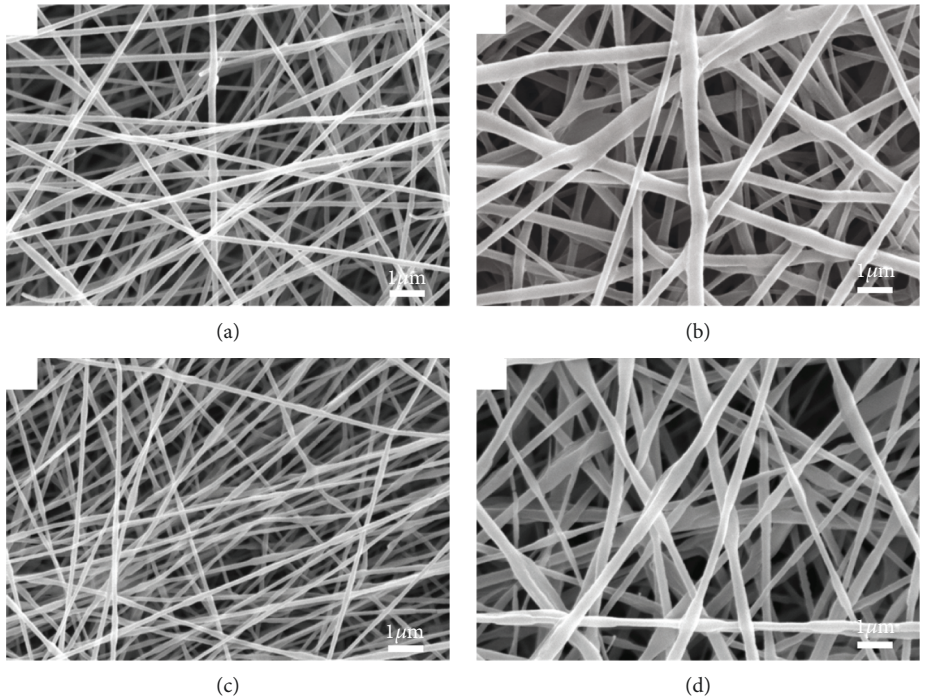

Figure 1: SEM images of (a) PLA, (b) PLA/PEO, (c) PLA/GSE, and (d) PLA/PEO/GSE nanofibers.

Table 1: Average fiber diameter and contact angle characterization of the nanofibrous membranes.

	PLA	PLA/PEO	PLA/GSE	PLA/PEO/GSE
Fiber diameter (nm)	149 ± 23	304 ± 46	130 ± 25	271 ± 66
Contact angle (°)	129 ± 4	58 ± 5	130 ± 3	46 ± 6
Contact angle images	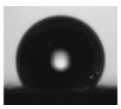		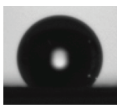	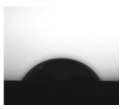

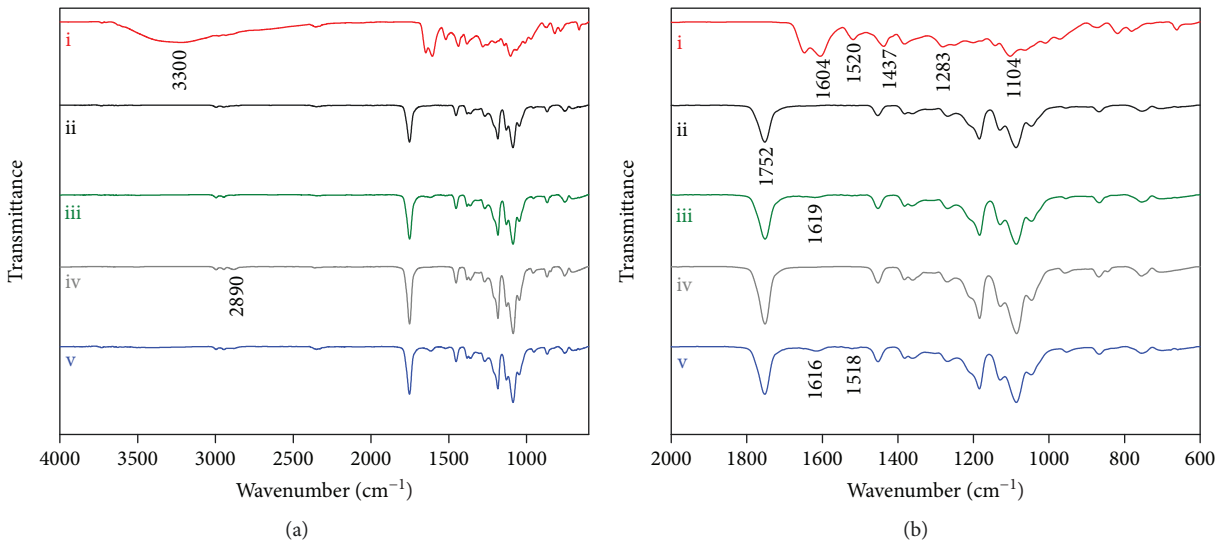

Figure 2: (a) FTIR spectra of (i) GSE powder and (ii) PLA, (iii) PLA/GSE, (iv) PLA/PEO, and (v) PLA/PEO/GSE nanofibers. (b) Close view in the range from 2000 to 600 cm^{-1}.

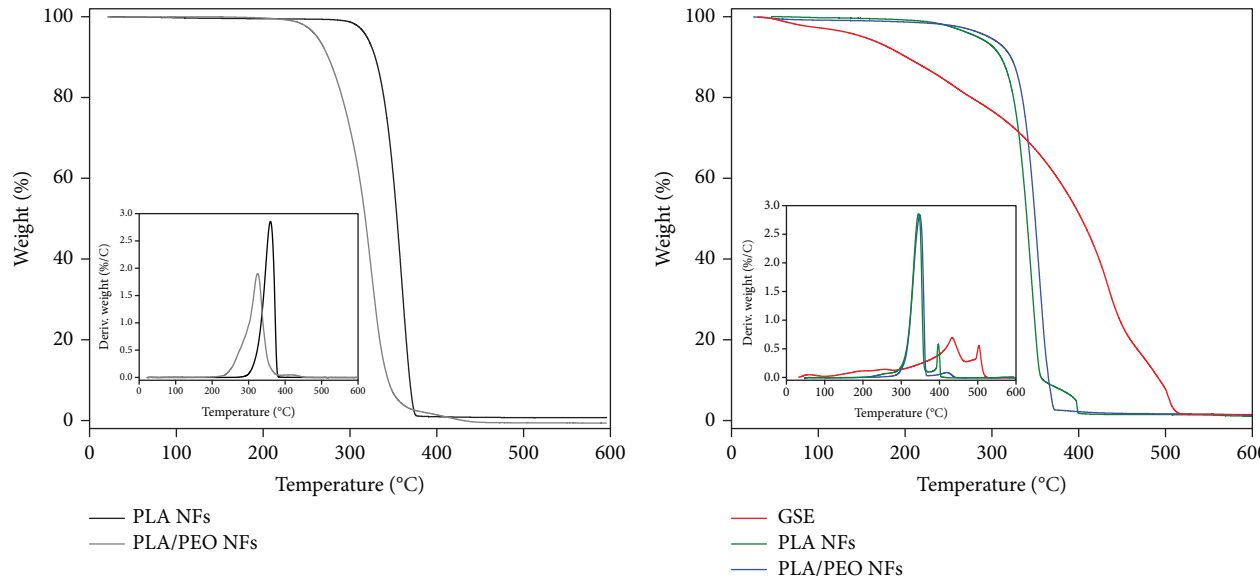

Figure 3: TG and DTG curves (inset) of (a) PLA and PLA/PEO and (b) GSE powder, PLA/GSE, and PLA/PEO/GSE nanofibers.

The biodegradability of PLA and PLA/PEO nanofibrous membranes was evaluated by monitoring their weight loss after soaking in PBS. The *in vitro* degradation profile (Figure 4(a)) over a period of 5 weeks showed around 9% degradation of PLA/PEO membranes owing to the presence of PEO [22]. For the same period of time, a negligible weight loss was detected for PLA nanofibrous membranes, showing the stability of the neat PLA membranes in PBS solution at pH 7.4. The low degradation rate of PLA can be a consequence of the low penetration and diffusion of water into the polymeric matrix owing to its hydrophobic nature [28], as corroborated by the contact angle data available in Table 1. SEM images after degradation tests showed that the morphology of both PLA (Figure 4(b)) and PLA/PEO (Figure 4(c)) membranes remained virtually unaffected. However, it was possible to observe an increase on PLA nanofiber diameters to 209 ± 60 nm due to the swelling and a decrease in the diameter of the PLA/PEO nanofibers to 260 ± 70 nm, which is in agreement with previous statements regarding the weight loss.

The encapsulation efficiency (EE) is an important parameter to evaluate the feasibility of clinical application of the developed material [44]. At the theoretical concentrations of 10%, the EE values of GSE were 88.4 ± 2.1 and 86.8 ± 1.7% for PLA and PLA/PEO nanofibers, respectively. These results indicated that there was virtually no loss of GSE during the electrospinning process and almost 90% of the extract could be encapsulated into the nanofibers using the electrospinning technique.

Reactive oxygen species (ROS) play a pivotal role in the expression of the normal wound healing response [45]. Generally, low levels of ROS are formed during the normal wound healing process for effective defense against invading pathogens and for intracellular signaling, especially for angiogenesis [46]. However, the presence of increased amounts of ROS could hamper the wound healing process by causing severe damage to the cells like fibroblasts, which secretes collagen and glycosaminoglycans for wound repair [47]. Hence, ROS scavenging properties of phenolic compounds might be important for the wound healing process.

GSE is well known to possess strong antioxidant potential and radical scavenging properties by countervailing harmful effects of ROS [13]. The antioxidant activity of GSE-loaded nanofibers was tested by using the DPPH radical scavenging assay. This method consists in performing reduction of the relatively stable DPPH radical to its nonradical form in the presence of a H-donating compound with antioxidant activity [31]. The antioxidant activity of the GSE for both loaded nanofibers (PLA/GSE and PLA/PEO/GSE) was determined as 85.5 ± 0.9%, even after 45 days. This result confirmed that the GSE retains its antioxidant activity after the electrospinning process and the nanofiber could efficiently protect the entrapped GSE from oxidation. Such result enables the application of our developed GSE-loaded nanofibrous membrane for biomedical materials to address oxidative stress issues.

3.2. In Vitro GSE Release Study. It is generally referred that the release rate of drug-loaded electrospun nanofibers can be modified by using different polymer combinations with distinct hydrophilic or hydrophobic nature [33]. In this way, the GSE release profile of PLA and PLA/PEO nanofibrous membranes was *in vitro* examined for a period of 30 days in PBS solution (pH 7.4) at 37°C, and the relationships between the cumulative percentage and releasing time were plotted in Figure 5. As can be seen, distinct GSE release profiles were observed from PLA and PLA/PEO membranes once brought into contact with PBS medium. The PLA nanofibrous membranes released about 60% of extract content after 24 h, but when the time was prolonged to 720 h,

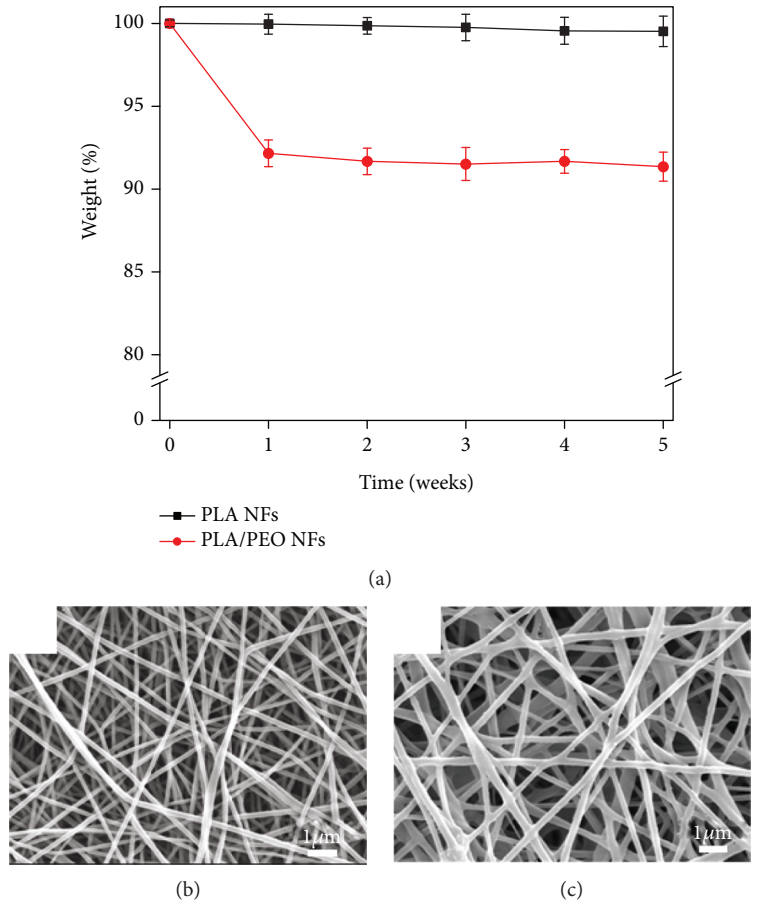

Figure 4: (a) *In vitro* degradation behavior of PLA and PLA/PEO membranes in PBS solution. SEM images of (b) PLA and (c) PLA/PEO nanofibers after 5 days of hydrolysis.

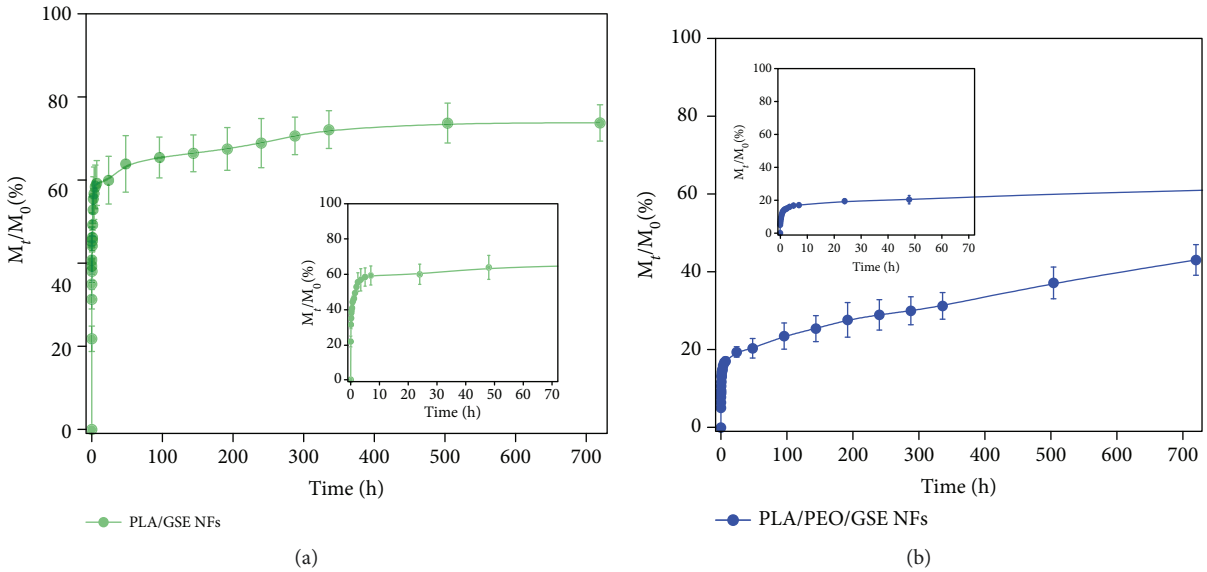

Figure 5: GSE *in vitro* release profiles from (a) PLA/GSE and (b) PLA/PEO/GSE nanofibrous membranes in a phosphate buffer solution (pH 7.4) at 37°C for 720 h. The insets show the close view of the release in the first 72 hours.

only an additional 4% content was released (Figure 5(a)). The initial burst release phenomenon is probably related to the drug entrapped near to the surface of the nanofibers, leading to a high initial drug delivery [44] that cannot persist for longer times. In contrast, PLA/PEO electrospun nanofibers exhibit a more sustained release pattern with a lower burst phenomenon, in which only about 20% of drug content was released over the same period of 24 h (Figure 5(b)).

The release of biomolecules loaded into nanofibrous membranes can be affected by several factors [3]. In general, the diffusion of the low molecular weight bioactive compound from fibrous materials depends on (1) the process of the membrane wetting and/or swelling, (2) the crystalline nature of the drug after the loading process, (3) the diffusion of water-soluble oligomers from the membranes, and (4) the nanofiber morphology [48]. In our case, the different behaviors presented by the blended nanofibers can be associated with the fact that the miscible mixtures of polymers propose a more sustained release pattern due to the difficulty of the drug to be diffused from the polymer matrix [37]. Additionally, the slower release rate for the PLA/PEO/GSE nanofibers can be attributed to the higher diameter of these nanofibers [33].

Several mathematical models have been used for studying the drug release profile from distinct polymer matrices [49]. Among them, the Korsmeyer-Peppas model (see equation (4) in Experiment) is widely used, since it can describe in a straightforward way the drug release profile from a polymeric system. This model categorizes release profiles based on the value of n exponent [35]. For $n \leq 0.5$, the model matches to a Fickian diffusion mechanism, while if n value lies between $0.5 < n < 1$, it is considered a non-Fickian (anomalous) mass transport mechanism [31]. Release kinetic parameter values (n and k) for GSE-loaded nanofibers are given in Table 2. The n value lower than 0.5 suggested that release of GSE from nanofibers showed a typical Fickian diffusion mechanism in which the release was caused by the concentration gradient between nanofibers and releasing medium [31].

3.3. In Vitro Cell Viability Evaluation. Fibroblasts are known to play a key role in the wound healing process by producing the majority of the extracellular matrix components and several cytokines and growth factors that are required for remodeling and wound closure [19]. The viability of FNN1 fibroblast cells on the pristine PLA and GSE-containing nanofibrous membranes was evaluated through the MTT cytotoxicity assay [50, 51], and the results are shown in Figure 6. It was found that the fibroblasts proliferated well in all the membranes, indicating that the nanofibrous membranes are nontoxic. After 24 h incubation, no significant difference in cell viability was noted between the different tested membranes. After 48 h, the results showed that the presence of GSE in both PLA and PLA/PEO membranes caused an improvement in the cell proliferation when compared to pristine PLA nanofibrous membranes, demonstrating the good cytocompatibility of GSE-loaded nanofibers. The enhancement in fibroblast activity after GSE addition can be related to the presence of proanthocyanidins in the extract [52]. These results suggested the promising effect of GSE loaded on nanofibrous membranes on the viability and growth of the fibroblast cells.

Table 2: Statistical parameters obtained from the *in vitro* release profiles through the Korsmeyer-Peppas model.

Sample	n	k (min^{-1})	R^2
PLA/GSE	0.16 ± 0.01	0.44 ± 0.03	0.985
PLA/PEO/GSE	0.29 ± 0.01	0.99 ± 0.06	0.989

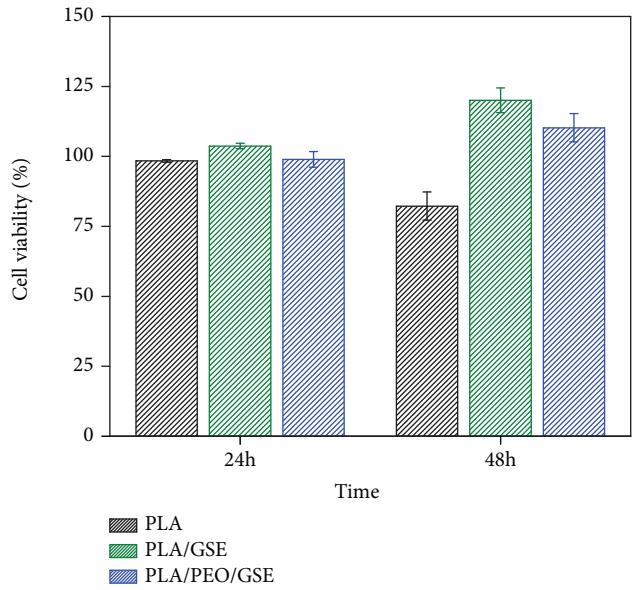

Figure 6: Viability of FNN1 fibroblast cells on PLA, PLA/GSE, and PLA/PEO/GSE nanofibrous membranes under different culture times (24 and 48 h).

In addition to cell viability investigation, the biocompatibility of a material is also related to the cell adhesion ability on the biomaterial surface [53]. Figure 7 shows the SEM images of fibroblast cells on the surface of nanofibrous membranes after 2 days of incubation. As can be seen, more cells were able to attach and grow on the PLA/PEO/GSE membrane, compared to the PLA/GSE membrane, as the former became more hydrophilic, which is suitable for cell adhesion [54]. Additionally, the cells attached on the surface of GSE-loaded PLA/PEO nanofibrous membranes achieved a more extended morphology, indicating higher cell affinity [47], compared to PLA membranes, which showed spherical morphology, indicating that they were still undifferentiated [54]. The results of the cell attachment and cytotoxicity study indicated that addition of PEO proved to be an excellent strategy to obtain a polymer membrane capable to support the attachment and proliferation of fibroblast cells with none or minimum cytotoxic effect. These results indicate that the fabricated GSE-loaded nanofibrous membranes present biocompatibility and can be considered as a safe alternative to be used as wound dressing materials.

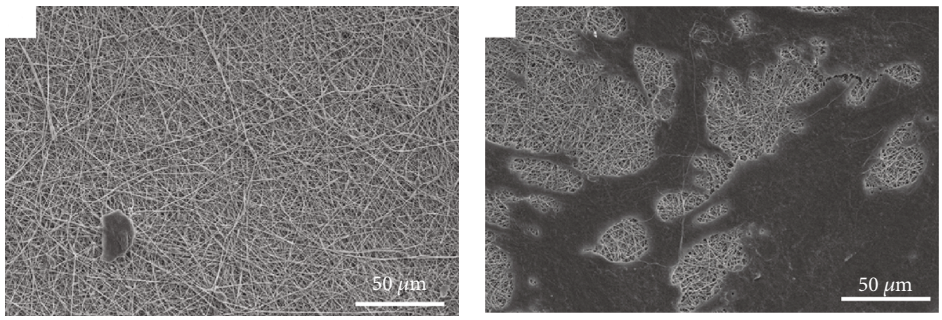

(a) (b)

Figure 7: SEM images of FNN1 fibroblast cells after 48 h cultured on (a) PLA/GSE and (b) PLA/PEO/GSE membranes.

4. Conclusion

In the present study, biocompatible and biodegradable nanofibrous membranes of PLA and PLA/PEO loaded with GSE have been successfully prepared by the electrospinning technique. FTIR and TG results showed that GSE was successfully encapsulated into the membranes, whose antioxidant activity was preserved. The GSE release profile from the polymer membranes showed to be dependent on the nanofiber composition, with a typical Fickian diffusion mechanism, where the addition of a hydrophilic polymer prolonged the GSE release period. Cell culture experiments with fibroblasts on the membranes demonstrated that the GSE-loaded samples are biocompatible and the addition of PEO proved to be able to support better cell adhesion and proliferation. Therefore, the developed nanofibrous membranes could be a suitable alternative platform for a new generation of antioxidant wound dressings.

Data Availability

The data used to support the findings of this study are included within the article.

Conflicts of Interest

The authors declare that they have no conflicts of interest.

Acknowledgments

The authors acknowledge the financial support from Fundação de Amparo à Pesquisa do Estado de São Paulo (FAPESP) (Grant numbers: 2016/23793-4 and 2017/12174-4), Conselho Nacional de Desenvolvimento Científico e Tecnológico (CNPq) (304109/2017-7 and 303.796/2014-6), Coordenação de Aperfeiçoamento de Pessoal de Nível Superior- (CAPES-) Brasil-Código de Financiamento 001, MCTI-SisNano (CNPq/402.287/2013-4), and Rede Agronano from Empresa Brasileira de Pesquisa Agropecuária (Embrapa) from Brazil.

References

[1] I. Sriyanti, D. Edikresnha, A. Rahma, M. M. Munir, H. Rachmawati, and K. Khairurrijal, "Correlation between structures and antioxidant activities of polyvinylpyrrolidone/-*Garcinia mangostana* L. extract composite nanofiber mats prepared using electrospinning," *Journal of Nanomaterials*, vol. 2017, Article ID 9687896, 10 pages, 2017.

[2] S. Lin, M. Chen, H. Jiang et al., "Green electrospun grape seed extract-loaded silk fibroin nanofibrous mats with excellent cytocompatibility and antioxidant effect," *Colloids Surfaces B: Biointerfaces*, vol. 139, pp. 156–163, 2016.

[3] M. Ignatova, N. Manolova, I. Rashkov, and N. Markova, "Antibacterial and antioxidant electrospun materials from poly(3-hydroxybutyrate) and polyvinylpyrrolidone containing caffeic acid phenethyl ester – "in" and "on" strategies for enhanced solubility," *International Journal of Pharmaceutics*, vol. 545, no. 1-2, pp. 342–356, 2018.

[4] M. J. Pérez, I. C. Zampini, M. R. Alberto, and M. I. Isla, "Prosopis nigra mesocarp fine flour, a source of phytochemicals with potential effect on enzymes linked to metabolic syndrome, oxidative stress, and inflammatory process," *Journal of Food Science*, vol. 83, no. 5, pp. 1454–1462, 2018.

[5] J. Merrell, S. McLaughlin, L. Tie, C. Laurencin, A. Chen, and L. Nair, "Curcumin loaded poly(ε-caprolactone) nanofibers: diabetic wound dressing with antioxidant and anti-inflammatory properties," *Clinical and Experimental Pharmacology and Physiology*, vol. 36, no. 12, pp. 1149–1156, 2009.

[6] G. Yakub, M. Ignatova, N. Manolova et al., "Chitosan/ferulic acid-coated poly(ε-caprolactone) electrospun materials with antioxidant, antibacterial and antitumor properties," *International Journal of Biological Macromolecules*, vol. 107, pp. 689–702, 2018.

[7] J. Wu, C. Omene, J. Karkoszka et al., "Caffeic acid phenethyl ester (CAPE), derived from a honeybee product propolis, exhibits a diversity of anti-tumor effects in pre-clinical models of human breast cancer," *Cancer Letters*, vol. 308, no. 1, pp. 43–53, 2011.

[8] M. G. Ignatova, N. E. Manolova, I. B. Rashkov et al., "Poly(3--hydroxybutyrate)/caffeic acid electrospun fibrous materials coated with polyelectrolyte complex and their antibacterial activity and in vitro antitumor effect against HeLa cells," *Materials Science and Engineering: C*, vol. 65, pp. 379–392, 2016.

[9] V. Silva, G. Igrejas, V. Falco et al., "Chemical composition, antioxidant and antimicrobial activity of phenolic compounds extracted from wine industry by-products," *Food Control*, vol. 92, pp. 516–522, 2018.

[10] N. Göktürk Baydar, G. Özkan, and S. Yaşar, "Evaluation of the antiradical and antioxidant potential of grape extracts," *Food Control*, vol. 18, no. 9, pp. 1131–1136, 2007.

[11] A. V. S. Perumalla and N. S. Hettiarachchy, "Green tea and grape seed extracts - potential applications in food safety and

quality," *Food Research International*, vol. 44, no. 4, pp. 827–839, 2011.

[12] K. Fernández, J. Aburto, C. Von Plessing, M. Rockel, and E. Aspé, "Factorial design optimization and characterization of poly-lactic acid (PLA) nanoparticle formation for the delivery of grape extracts," *Food Chemistry*, vol. 207, pp. 75–85, 2016.

[13] M. Gibis, C. Ruedt, and J. Weiss, "*In vitro* release of grape-seed polyphenols encapsulated from uncoated and chitosan-coated liposomes," *Food Research International*, vol. 88, Part A, pp. 105–113, 2016.

[14] A. Barras, A. Mezzetti, A. Richard et al., "Formulation and characterization of polyphenol-loaded lipid nanocapsules," *International Journal of Pharmaceutics*, vol. 379, no. 2, pp. 270–277, 2009.

[15] R. Schneider, L. A. Mercante, R. S. Andre, H. d. M. Brandão, L. H. C. Mattoso, and D. S. Correa, "Biocompatible electrospun nanofibers containing cloxacillin: antibacterial activity and effect of pH on the release profile," *Reactive and Functional Polymers*, vol. 132, pp. 26–35, 2018.

[16] S. P. Miguel, D. R. Figueira, D. Simões et al., "Electrospun polymeric nanofibres as wound dressings: a review," *Colloids Surfaces B: Biointerfaces*, vol. 169, pp. 60–71, 2018.

[17] H. Cheng, X. Yang, X. Che, M. Yang, and G. Zhai, "Biomedical application and controlled drug release of electrospun fibrous materials," *Materials Science and Engineering: C*, vol. 90, pp. 750–763, 2018.

[18] P. Wen, M. H. Zong, R. J. Linhardt, K. Feng, and H. Wu, "Electrospinning: a novel nano-encapsulation approach for bioactive compounds," *Trends in Food Science and Technology*, vol. 70, pp. 56–68, 2017.

[19] C. H. Yao, J. Y. Yeh, Y. S. Chen, M. H. Li, and C. H. Huang, "Wound-healing effect of electrospun gelatin nanofibres containing Centella asiatica extract in a rat model," *Journal of Tissue Engineering and Regenerative Medicine*, vol. 11, no. 3, pp. 905–915, 2017.

[20] S. Xin, X. Li, Q. Wang et al., "Novel layer-by-layer structured nanofibrous mats coated by protein films for dermal regeneration," *Journal of Biomedical Nanotechnology*, vol. 10, no. 5, pp. 803–810, 2014.

[21] F. Ding, H. Deng, Y. Du, X. Shi, and Q. Wang, "Emerging chitin and chitosan nanofibrous materials for biomedical applications," *Nanoscale*, vol. 6, no. 16, pp. 9477–9493, 2014.

[22] T. T. Yuan, P. M. Jenkins, A. M. DiGeorge Foushee, A. R. Jockheck-Clark, and J. M. Stahl, "Electrospun chitosan/polyethylene oxide nanofibrous scaffolds with potential antibacterial wound dressing applications," *Journal of Nanomaterials*, vol. 2016, Article ID 6231040, 10 pages, 2016.

[23] J. Li, Y. Hu, T. He et al., "Electrospun sandwich-structure composite membranes for wound dressing scaffolds with high antioxidant and antibacterial activity," *Macromolecular Materials and Engineering*, vol. 303, no. 2, pp. 1–13, 2018.

[24] H. Zhou, X. Liu, F. Wu et al., "Preparation, characterization, and antitumor evaluation of electrospun resveratrol loaded nanofibers," *Journal of Nanomaterials*, vol. 2016, Article ID 5918462, 11 pages, 2016.

[25] S. Honarbakhsh and B. Pourdeyhimi, "Scaffolds for drug delivery, part I: electrospun porous poly(lactic acid) and poly(lactic acid)/poly(ethylene oxide) hybrid scaffolds," *Journal of Materials Science*, vol. 46, no. 9, pp. 2874–2881, 2011.

[26] M. Santoro, S. R. Shah, J. L. Walker, and A. G. Mikos, "Poly(lactic acid) nanofibrous scaffolds for tissue engineering," *Advanced Drug Delivery Reviews*, vol. 107, pp. 206–212, 2016.

[27] T. T. Yuan, A. Marie, D. Foushee, M. C. Johnson, A. R. Jockheck-clark, and J. M. Stahl, "Development of electrospun chitosan-polyethylene oxide/fibrinogen biocomposite for potential wound healing applications," *Nanoscale Research Letters*, vol. 13, no. 1, p. 88, 2018.

[28] A. Oyarzabal, A. Mugica, A. J. Müller, and M. Zubitur, "Hydrolytic degradation of nanocomposites based on poly (L-lactic acid) and layered double hydroxides modified with a model drug," *Journal of Applied Polymer Science*, vol. 133, no. 28, pp. 2–11, 2016.

[29] P. Chuysinuan, N. Chimnoi, S. Techasakul, and P. Supaphol, "Gallic acid-loaded electrospun poly(L-lactic acid) fiber mats and their release characteristic," *Macromolecular Chemistry and Physics*, vol. 210, no. 10, pp. 814–822, 2009.

[30] M. Yourdkhani, A. A. Leme-Kraus, B. Aydin, A. K. Bedran--Russo, and S. R. White, "Encapsulation of grape seed extract in polylactide microcapsules for sustained bioactivity and time-dependent release in dental material applications," *Dental Materials*, vol. 33, no. 6, pp. 630–636, 2017.

[31] A. Altan, Z. Aytac, and T. Uyar, "Carvacrol loaded electrospun fibrous films from zein and poly(lactic acid) for active food packaging," *Food Hydrocolloids*, vol. 81, pp. 48–59, 2018.

[32] C. Mellado, T. Figueroa, R. Báez et al., "Development of graphene oxide composite aerogel with proanthocyanidins with hemostatic properties as a delivery system," *ACS Applied Materials & Interfaces*, vol. 10, no. 9, pp. 7717–7729, 2018.

[33] P. I. Siafaka, P. Barmbalexis, and D. N. Bikiaris, "Novel electrospun nanofibrous matrices prepared from poly(lactic acid)/poly(butylene adipate) blends for controlled release formulations of an anti-rheumatoid agent," *European Journal of Pharmaceutical Sciences*, vol. 88, pp. 12–25, 2016.

[34] H. Wang, L. Hao, B. Niu, S. Jiang, J. Cheng, and S. Jiang, "Kinetics and antioxidant capacity of proanthocyanidins encapsulated in zein electrospun fibers by cyclic voltammetry," *Journal of Agricultural and Food Chemistry*, vol. 64, no. 15, pp. 3083–3090, 2016.

[35] P. Dubey and P. Gopinath, "Fabrication of electrospun poly (ethylene oxide)-poly(capro lactone) composite nanofibers for co-delivery of niclosamide and silver nanoparticles exhibits enhanced anti-cancer effects in vitro," *Journal of Materials Chemistry B*, vol. 4, no. 4, pp. 726–742, 2016.

[36] M. G. Ignatova, N. E. Manolova, R. a. Toshkova et al., "Electrospun nanofibrous mats containing quaternized chitosan and polylactide with in vitro antitumor activity against HeLa cells," *Biomacromolecules*, vol. 11, no. 6, pp. 1633–1645, 2010.

[37] R. Dai and L. T. Lim, "Release of allyl isothiocyanate from mustard seed meal powder entrapped in electrospun PLA-PEO nonwovens," *Food Research International*, vol. 77, pp. 467–475, 2015.

[38] J. Nogales-Bueno, B. Baca-Bocanegra, A. Rooney, J. M. Hernández-Hierro, H. J. Byrne, and F. J. Heredia, "Study of phenolic extractability in grape seeds by means of ATR-FTIR and Raman spectroscopy," *Food Chemistry*, vol. 232, pp. 602–609, 2017.

[39] B. W. Chieng, N. A. Ibrahim, W. M. Z. W. Yunus, and M. Z. Hussein, "Plasticized poly(lactic acid) with low molecular weight poly(ethylene glycol): mechanical, thermal, and morphology properties," *Journal of Applied Polymer Science*, vol. 130, pp. 4576–4580, 2013.

[40] M. Brebu, J. Yanik, T. Uysal, and C. Vasile, "Thermal and catalytic degradation of grape seeds/polyethylene waste mixture," *Cellulose Chemistry and Technology*, vol. 48, no. 7-8, pp. 665–674, 2014.

[41] E. Părpăriță, M. T. Nistor, M. C. Popescu, and C. Vasile, "TG/FT–IR/MS study on thermal decomposition of polypropylene/biomass composites," *Polymer Degradation and Stability*, vol. 109, pp. 13–20, 2014.

[42] M. Aceituno-Medina, S. Mendoza, B. A. Rodríguez, J. M. Lagaron, and A. López-Rubio, "Improved antioxidant capacity of quercetin and ferulic acid during in-vitro digestion through encapsulation within food-grade electrospun fibers," *Journal of Functional Foods*, vol. 12, pp. 332–341, 2015.

[43] D. Kai, K. Zhang, L. Jiang et al., "Sustainable and antioxidant lignin-polyester copolymers and nanofibers for potential healthcare applications," *ACS Sustainable Chemistry & Engineering*, vol. 5, no. 7, pp. 6016–6025, 2017.

[44] M. Cheng, Z. Qin, S. Hu, S. Dong, Z. Ren, and H. Yu, "Achieving long-term sustained drug delivery for electrospun biopolyester nanofibrous membranes by introducing cellulose nanocrystals," *ACS Biomaterials Science & Engineering*, vol. 3, no. 8, pp. 1666–1676, 2017.

[45] C. Dunnill, T. Patton, J. Brennan et al., "Reactive oxygen species (ROS) and wound healing: the functional role of ROS and emerging ROS-modulating technologies for augmentation of the healing process," *International Wound Journal*, vol. 14, no. 1, pp. 89–96, 2017.

[46] C. Mohanty and S. K. Sahoo, "Curcumin and its topical formulations for wound healing applications," *Drug Discovery Today*, vol. 22, no. 10, pp. 1582–1592, 2017.

[47] S. Selvaraj and N. N. Fathima, "Fenugreek incorporated silk fibroin nanofibers - a potential antioxidant scaffold for enhanced wound healing," *ACS Applied Materials & Interfaces*, vol. 9, no. 7, pp. 5916–5926, 2017.

[48] I. Sebe, P. Szabó, B. Kállai-Szabó, and R. Zelkó, "Incorporating small molecules or biologics into nanofibers for optimized drug release: a review," *International Journal of Pharmaceutics*, vol. 494, no. 1, pp. 516–530, 2015.

[49] P. Costa and J. M. Sousa Lobo, "Modeling and comparison of dissolution profiles," *European Journal of Pharmaceutical Sciences*, vol. 13, no. 2, pp. 123–133, 2001.

[50] C. Gao, F. Tang, G. Gong et al., "PH-responsive prodrug nanoparticles based on a sodium alginate derivative for selective co-release of doxorubicin and curcumin into tumor cells," *Nanoscale*, vol. 9, no. 34, pp. 12533–12542, 2017.

[51] C. Gao, F. Tang, J. Zhang, S. M. Y. Lee, and R. Wang, "Glutathione-responsive nanoparticles based on a sodium alginate derivative for selective release of doxorubicin in tumor cells," *Journal of Materials Chemistry B*, vol. 5, no. 12, pp. 2337–2346, 2017.

[52] M. Tsuruya, Y. Niwano, K. Nakamura et al., "Acceleration of proliferative response of mouse fibroblasts by short-time pretreatment with polyphenols," *Applied Biochemistry and Biotechnology*, vol. 174, no. 6, pp. 2223–2235, 2014.

[53] R. Huang, W. Li, X. Lv et al., "Biomimetic LBL structured nanofibrous matrices assembled by chitosan/collagen for promoting wound healing," *Biomaterials*, vol. 53, pp. 58–75, 2015.

[54] J. Hu, D. Kai, H. Ye et al., "Electrospinning of poly(glycerol sebacate)-based nanofibers for nerve tissue engineering," *Materials Science and Engineering: C*, vol. 70, Part 2, pp. 1089–1094, 2017.